

## Experimental determination of S/XB values of Sn I emission lines in GyM device

A. Cremona<sup>1</sup>, A. Uccello<sup>1</sup>, F. Causa<sup>1</sup>, R. Caniello<sup>1</sup>, S. De Iuliis<sup>2</sup>, R. Dondè<sup>2</sup>, G. Gervasini<sup>1</sup>,  
F. Ghezzi<sup>1</sup>, G. Granucci<sup>1</sup>, L. Laguardia<sup>1</sup>, V. Mellera<sup>1</sup>, D. Minelli<sup>1,3</sup>, A. Nardone<sup>1</sup>,  
M. Pedroni<sup>1</sup>, D. Ricci<sup>1</sup>, N. Rispoli<sup>1</sup>, E. Vassallo<sup>1</sup>

<sup>1</sup>CNR, Istituto di Fisica del Plasma Piero Caldirola, Milano, Italy

<sup>2</sup>CNR, Istituto di Chimica della Materia Condensata e di Tecnologie per l'Energia, Milano, Italy

<sup>3</sup>EPFL, Swiss Plasma Center, Lausanne, Switzerland

**Introduction** The recent demand of heat handling on materials compatible with the harsh environments of fusion reactors has led to increased efforts into materials research. The high heat load afforded by liquid metals together with their regenerative properties and resilience to neutron damage make them eminently suitable for use as Plasma Facing Components (PFCs). Among liquid metals tin (Sn) is a valid candidate because it presents low vapour pressure and low reactivity with hydrogen; however, it is also characterised by a high atomic number,  $Z = 50$ , which causes concerns about plasma contamination.

Optical Emission Spectroscopy (OES) is an optical plasma diagnostics that can be used to estimate impurity influx through the S/XB spectroscopic parameter, [1]. The aim of this work is the spectroscopic determination of the S/XB factor for Sn I line at 380.1 nm in GyM device through the empiric evaluation of the mass loss. Two different magnetic configurations have been exploited to permit the exposure of both solid and liquid Sn samples. In particular, a linear magnetic configuration was used to expose solid samples and a double-cusp configuration for liquid samples without making use of the capillary porous system (CPS).

**Experimental** Solid and liquid Sn samples were exposed to Ar plasma in GyM, at operating pressures ranging from  $2 \times 10^{-5}$  to  $1 \times 10^{-4}$  mbar. A schematic of GyM is presented in Figure 1. GyM consists of a stainless steel vacuum chamber ( $\mathcal{O} = 0.25$  m, length 2.11 m) mounted in a solenoid with a magnetic field of 0.08 T on axis. Plasmas are generated and continuously sustained by means of RF power (3 kW CW) in the electron cyclotron frequency range (2.45 GHz). Solid Sn, placed in a sample holder tilted by 45°, was inserted in the vessel using a linear magnetic field configuration, Figure 2(a). A negative bias,  $V_{applied} = -100$  V, was applied to achieve incident ion energy of  $\sim 50$ -70 eV, taking into account also

the plasma potential ( $V_p \sim 30\text{-}50$  V). On the other hand, to expose liquid Sn samples without the use of CPS, a double-cusp magnetic configuration, Figure 2(b), obtained by current inversion in two coils, was used.

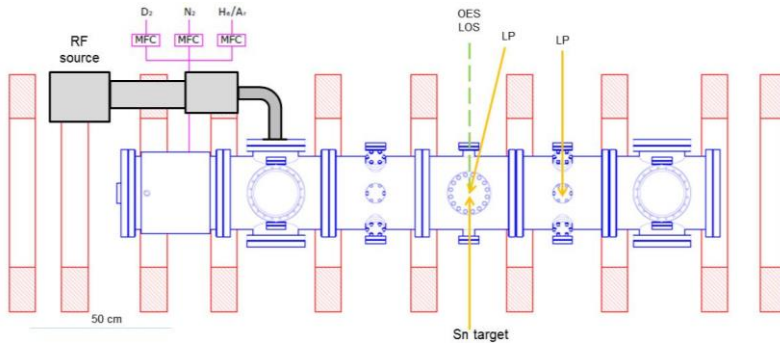


**Figure 1: Schematic of the plasma GyM device.**

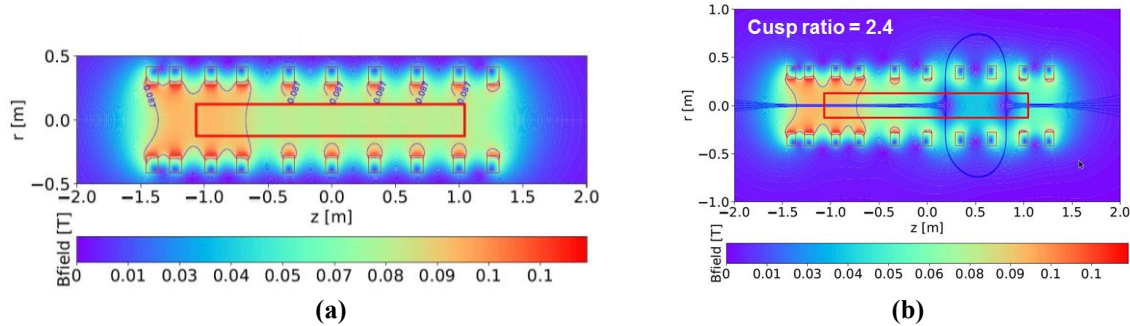


**Figure 2. The two magnetic configurations used to expose solid and liquid Sn samples: (a) linear and (b) double-cusp configuration.**

**GyM plasma parameters** Two diagnostics are available for the evaluation of plasma parameters in GyM: Langmuir Probe (LP) and Optical Emission Spectroscopy (OES). In particular, OES presents a line of sight (LOS) perpendicular to the machine axis, and the resulting parameters are LOS-integrated. With OES the electron density  $n_e$  is obtained from the ratio of emission line coefficients (PECs) of Ar II lines (480.6 nm and 488.0 nm) [2]:

$$(1) \quad \frac{I_{480.6}}{I_{488.0}} = \frac{PEC_{480.6}}{PEC_{488.0}}$$

and the electron temperature  $T_e$  from the absolute intensity of Ar I line at 750.4 nm [3]:

$$(2) \quad I_{750.4} = n_0 n_e PEC(T_e)$$

In both equations (1) and (2), PECs are taken from ADAS database [4].

Part of the study was devoted to the benchmarking of the OES measured values with respect to those obtained with the LP. Preliminary results are promising. In particular, for the linear magnetic configuration, results for the electron density are typically higher for OES by a

factor  $f_{ne} = 2$ , while results for  $T_e$  are in good quantitative agreement, Figure 3(a). In the double-cusp configuration,  $f_{ne} = 3.5$ , and results for  $T_e$  are in good quantitative agreement for values on axis, Figure 3(b).

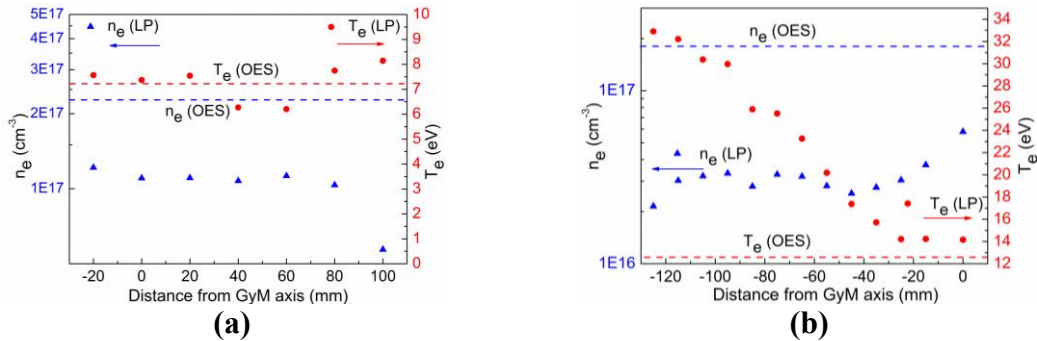


Figure 3: Plasma parameters, electron density (blue) and temperature (red) estimated using LP (symbols) and OES (dashed lines) in the (a) linear and (b) double-cusp configurations.

### Evaluation of the S/XB spectroscopic parameter

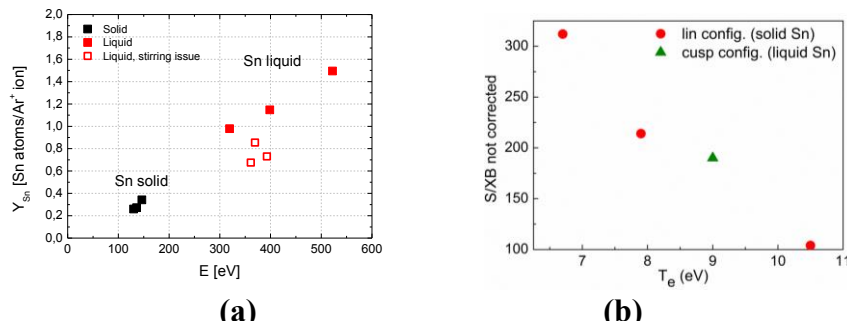
S/XB is a spectroscopic parameter converting emission line intensity into an influx of Sn impurity atoms from limiting surfaces, i.e., the ionization (S) per excitation rate (X) corrected for the branching ratio (B). In GyM only a fraction of Sn sputtered atoms is ionized in the plasma, so that the flux of sputtered atoms is represented as  $\Gamma_{Sn}^{Sputt} = \Gamma_{Sn \rightarrow Sn^+} + \Gamma_{Sn}^{GL}$ , where  $\Gamma_{Sn \rightarrow Sn^+} = 4\pi \frac{S}{XB} I_{SnI}$  is the ionization flux,  $I_{SnI}$  the absolute line-integrated intensity of sputtered Sn atoms and  $\Gamma_{Sn}^{GL}$  the geometric loss flux. Equivalently, the sputtered flux can be written as  $\Gamma_{Sn}^{Sputt} = Y_{Sn} \Gamma_i$ , where  $Y_{Sn}$  is the sputtering yield determined by mass loss measurements and  $\Gamma_i$  is the incident ion

flux, so that S/XB parameter is calculated as  $\frac{S}{XB} = \frac{1}{4\pi I_{Sn}} \Gamma_{Sn}^{Sputt} \left(1 - \frac{\Gamma_{Sn}^{GL}}{\Gamma_{Sn}^{Sputt}}\right)$  where the geometric correction factor is evaluated as  $\frac{\Gamma_{Sn}^{GL}}{\Gamma_{Sn}^{Sputt}} \approx e^{-\frac{L}{\lambda_{mfp}}}$  with  $L$  = characteristic length of

the system, i.e., the minimum escape length of Sn sputtered atoms and  $\lambda_{mfp}$  = ionization mean free path of Sn atoms. Experimental results for sputtering yield, presented in Figure 4 (a), are in line with data presented in the literature for liquid and solid tin, [6-7]. Experimental results for S/XB for Ar I line at 380.1 nm and the corresponding geometric loss correction factor are presented in Table 1 and Figure 4 (b). The order of magnitude of the S/XB obtained in linear configuration for Sn is consistent with that obtained for W in PISCES-B, [5]. However, more effort is needed for an accurate evaluation of the geometric loss flux in both experimental configurations.

**Table 1: Geometric loss factor evaluated using LP/OES-estimated plasma parameters.**

Magnetic configuration	T <sub>e</sub> (eV)	S/XB	Geometric loss correction n <sub>e</sub> ~ 1-2 × 10 <sup>11</sup> cm <sup>-3</sup>
Linear (solid Sn)	10.5	104	0.7 - 0.9
Linear (solid Sn)	7.9	214	0.6 - 0.8
Linear (solid Sn)	6.7	312	0.5 - 0.7
Cusp (liquid Sn)	9	190	0.9 (n <sub>e</sub> ~ 2 × 10 <sup>11</sup> cm <sup>-3</sup> )

**Figure 4. (a) Sn sputtering yield, and (b) experimental results for S/XB for the Sn I line at 380.1 nm.**

**Conclusion** Experimental results for S/XB in linear configuration are in qualitative agreement with those obtained in PISCES-B for W. The calculated sputtering yield is in line with results presented in the literature for liquid and solid Sn. The cusp magnetic configuration is used here for the first time to expose liquid Sn, making GyM suitable for the study of solid and liquid metals. More effort is needed for an accurate evaluation of the geometric loss flux in both experimental configurations. Further tests are needed to benchmark OES against LP to estimate plasma parameters.

## References

- [1] K. Behringer *et al.*, Plasma Phys. and Control Fus 31, 2059, 1989
- [2] U. Fantz *et al.*, Nucl. Fus 46, S297, 2006
- [3] U. Fantz *et al.*, Plasma Sources Sci. Technol. 15, S137, 2006
- [4] H. Summers *et al.*, <http://open.adas.ac.uk/adf15>, University of Strathclyde, Glasgow
- [5] D. Nishijima *et al.*, Physics of Plasmas 16, 122503, 2009
- [6] R.C. Krutenat *et al.*, JAP 41, 4953, 1970
- [7] G.K. Wehner *et al.*, Phys. Rev. 102, 690, 1956

## Acknowledgement

*This work has been carried out within the framework of the EUROfusion Consortium and has received funding from the Euratom research and training programme 2014-2018 under grant agreement No 633053. The views and opinions expressed herein do not necessarily reflect those of the European Commission.*

*Work performed under EUROfusion WP PFC.*